



Rational design and *in-vivo* estimation of Ivabradine Hydrochloride loaded nanoparticles for management of stable angina

Vipin Sharma^a, Hitesh Kumar Dewangan^b, Lakshmi Maurya^a, Kanchan Vats^c, Himanshu Verma^a, Sanjay Singh Professor^{a,*}

^a Department of Pharmaceutical Engineering and Technology, Indian Institute of Technology, Banaras Hindu University, Varanasi, 221005, India

^b Institute of Pharmaceutical Research (IPR), GLA University, Mathura, 281406, India

^c National Institute of Pharmaceutical Education and Research (NIPER), Gandhinagar-382355, Gujarat, India

ARTICLE INFO

Keywords:

Stable angina
Ivabradine hydrochloride
Polymeric nanoparticles
Box-behnken design
Anti-anginal activity

ABSTRACT

Stable angina or angina pectoris is referred to as uneasiness/pain in the chest, resulting from coronary heart disease (CHD). Ivabradine Hydrochloride (IBH) is a recently approved drug to manage stable angina and heart failure symptoms. The approved IBH tablets exhibit some technical shortcomings i.e. short half-life (2 h), variable systemic absorption, and high first-pass metabolism (> 50%). Therefore, utilizing a nanoformulation technique, we have designed a differentiated and innovative formulation of IBH. The IBH loaded polymeric nanoparticles (IBH-PNPs) are being developed for per-oral delivery by double emulsion method, using Poly lactic-co-glycolic acid (PLGA) as polymer, and D- α -tocopherol polyethylene glycol 1000 succinate (TPGS) as a stabilizer. The pre-formulation studies performed are UV spectroscopy, FT-IR, and X-ray diffraction. The Box-Behnken design was exploited for formulation optimization. The optimized formulation was characterized for its particle size, zeta potential, morphology, entrapment efficiency, *in-vitro* release, stability studies, *ex-vivo* permeability, and *in-vivo* pharmacodynamics study. The optimized IBH-PNPs were found to be spherical (< 200nm) and exhibited normal size distribution under transmission electron microscopy and atomic force microscopy respectively. The zeta potential and entrapment efficiency were found to be -43.75 mv and $60 \pm 4.8\%$ respectively. Developed IBH-PNPs analyzed for *in-vitro* drug release where they exhibited biphasic release. The *ex-vivo* drug permeation study showed 1.85 folds increment in intestinal permeability as compared to IBH tablets. The *in-vivo* anti-anginal efficacy studies were performed using vasopressin-induced angina model in Wistar rats. Developed formulation was found to have a therapeutic effect for three days.

1. Introduction

Coronary heart diseases (CHD) are a matter of concern for the globe due to rising mortality and morbidity cases. The deaths and disabilities due to CHD are increasing continuously in developing countries; however, declining in developed countries [1]. According to the World Health Organization (WHO), South Asia region has one of the highest CHD mortality rates in the world [2,3]. Stable angina is one of the outcomes of CHD that causes uneasiness/pain in the chest. It arises when cardiac muscles do not get enough blood supply; one or more blood arteries gets narrowed or blocked. Angina causes pain and discomfort in the neck, jaw, shoulder, back or arm.

Ivabradine Hydrochloride (IBH) is a recently approved medicine for

stable angina and chronic heart failure management-lowering the heart rate. It works by inhibiting “funny channels” present in SA-node. In 2005, IBH tablets were approved by the European Medicines Agency; US FDA in 2015. The marketed dosage form (tablet) was found to have the following technical setbacks: oral bioavailability (35%–40%), half-life (2 h), and First pass metabolism (> 50%) by enzyme CYP3A4. As far as safety is concerned, the clinical trials of the approved product have shown the following side effects: bradycardia, hypertension, atrial fibrillation, temporary vision disturbance (flashes of light), dizziness, weakness or fatigue. In order to solve the aforementioned unmet needs, we have come up with a new strategy i.e. Ivabradine Hydrochloride loaded polymeric nanoparticles (IBH-PNPs). Polymeric nanoparticles could be an alternative to reduce the drawbacks associated with IBH

* Corresponding author. Department of Pharmaceutical Engineering and Technology, Indian Institute of Technology, Banaras Hindu University, Varanasi, 221005, India.

E-mail addresses: vipins.phe16@itbhu.ac.in (V. Sharma), hitesh.dewangan@gla.ac.in (H.K. Dewangan), laxmi.rs.phe13@itbhu.ac.in (L. Maurya), vats.kanchan32@gmail.com (K. Vats), himanshuv.phe16@itbhu.ac.in (H. Verma), ssingh.phe@iitbhu.ac.in (S. Singh).

<https://doi.org/10.1016/j.jddst.2019.101337>

Received 17 August 2019; Received in revised form 6 October 2019; Accepted 19 October 2019

Available online 20 November 2019

1773-2247/ © 2019 Elsevier B.V. All rights reserved.

tablet. The polymeric nanoparticles are more stable in GIT, avoiding first-pass metabolism, would release the drug in a sustained manner in systemic circulation via lymphatic transport [5,23]. The use of several polymeric materials enables the manipulation of physiological (surface property, hydrophobicity, drug release properties) and biological characteristics (targeting, bio-adhesion, improved cellular uptake) of nanoparticles [6,22]. Hence, this work was aimed to prepare polymeric nanoparticles of Ivabradine Hydrochloride (IBH-PNPs) by double-emulsion solvent evaporation method; using Poly lactic-co-glycolic acid (PLGA) as polymer and D- α -tocopherol polyethylene glycol 1000 succinate (TPGS) as a surfactant. The 3-level, 3-factor Box-Behnken experimental design was utilized for the understanding of the effect of independent (Polymer amount, TPGS concentration, Organic/Aqueous ratio) process variables and formulation variables on dependent variables (i.e. particle size, entrapment efficiency, and zeta potential). Further, the optimized IBH-PNPs was characterized for various physicochemical properties like particle size, zeta potential, morphology, Stability studies, *in-vitro* studies, *ex-vivo* intestinal permeation study, and *in-vivo* anti-anginal activity in Wistar rats.

2. Materials and methods

Ivabradine Hydrochloride was received as a gift sample from Ind-Swift Labs Ltd, Jammu & Kashmir, India. PLGA (RG750S) and TPGS were procured as a kind gift sample from Evonic Degussa India Pvt. Ltd., Mumbai, India and Antares Health products Inc. (St. Charles, Illinois, USA) respectively. Other chemicals (Tween 80 and Span 80) and solvent (Dichloromethane) were of analytical grade; purchased from SD fine chemicals, Mumbai, India. Distilled water (by Sartorius water purifier system) was used in all the studies.

2.1. Methods

2.1.1. Preparation of IBH-PNPs

The IBH-PNPs were fabricated by the double-emulsion solvent evaporation method (w/o/w), with a minor modification in the method developed by Zambaux et al., 1998 [30]. Firstly, organic phase was prepared by dissolving PLGA and Span 80 in organic solvent (dichloromethane). Next, the drug solution was obtained by adding IBH in distilled water. Then, under probe sonication (60% amplitude and 0.6 s frequencies), drug solution was added into the organic phase to obtain primary emulsion (w/o). Finally, the primary emulsion was added dropwise into TPGS-water solution using a syringe (26 G, 0.45 mm internal diameter) under homogenization (IKA T25 digital Ultra Turrax, Germany) to obtain secondary emulsion (w/o/w). The prepared emulsion was kept on magnetic stirring overnight for the evaporation of the organic solvent. The obtained nanoparticles were centrifuged (Cooling centrifuge, Remi Instrument Pvt. LTD., India) at 15000 rpm for 20 min at -4°C to remove the untrapped drug and free TPGS. The washed nanoparticles were lyophilized (LFD-BT-101, Labocoon Freeze Dryer) for 32 h in presence of lyoprotectant (mannitol 5 w/v) to obtain dried nanoparticles.

2.1.2. Formulation optimization by Box-Behnken experimental design

Response surface methodology (RSM) was applied for the statistical optimization of the IBH-PNPs. The RSM is an important tool devoted to design, model, and evaluate the impact of variables statistically. In the present study, a response surface model (RSM), 3-level, 3-factor, Box-Behnken experimental design (using Design-Expert Software® 7.0.0) was utilized for optimization and establishing a relationship between independent and dependent variables.

Based on preliminary studies, the polymer amount (A), TPGS concentration (B), and Organic phase/aqueous phase ratio (C) were found as critical variables. These variables were varied at three levels: +1 (high), 0 (medium), -1 (low) as summarized in Table 1. The total number of experiments (N) required for the generation of the design

Table 1
Dependent and independent variables and their corresponding levels.

Independent variables	Coded levels of variables		
	Low (-1)	Medium (0)	High ($+1$)
A = Polymer amount (mg)	20	25	30
B = TPGS concentration (%w/v)	0.05	0.1	0.15
C = Organic/aqueous ratio (v/v)	0.33	0.5	0.66

Dependent variables	Constraints
Particle size (nm)	Minimize
Entrapment efficiency (%)	Maximize
Polydispersity index (PDI)	Minimize

matrix of Box-Behnken experimental design was decided by considering the following formula:

$$n = 2k(k-1) + C_0$$

Where k is the number of variables; C_0 refers to the number of center points.

The BBD suggested 17 experiments, which were conducted in a randomized manner to eliminate any possible chance of error; thus, eliminating variability and biases of the response (Table 1). The effect of independent variables was analyzed using the following non-linear polynomial equation:

$$y = B_0 + B_1X_1 + B_2X_2 + B_3X_3 + B_4X_1X_3 + B_6X_1X_3 + B_6X_1X_3 + B_7X_1^2 + B_8X_2^2 + B_9X_3^2 + E$$

Here y is measured response; B_0 is an intercept; B_1 – B_9 are the regression coefficients; B_1 – B_3 are the main effect of X_1 – X_3 ; B_4 – B_6 is the interactive effect of main factors; B_7 – B_9 are the quadratic effects of the independent variables, and E is the random error term [1,19].

2.1.3. Physicochemical characterization

The particle size and PDI of prepared IBH-PNPs were determined by Delsa-Nano C particle size analyzer (Beckman Coulter, UK) which works on the principle of photon correlation spectroscopy. The measurements were performed at a fixed angle of 165° at 25°C temperature, using scattering light generated by standard He–Ne laser. The zeta potential of IBH-PNPs was determined under the influence of an applied electric field by measuring the electrophoretic mobility of charged particles. IBH-PNPs were diluted and sonicated before all measurements [1].

The surface properties of IBH-PNPs were examined employing transmission electron microscopy (TEM), atomic force microscopy (AFM). For AFM, the sample (5–10 μl) was deposited on fresh glass cover slip and allowed to be air dried to obtain a thin film, then observed in AFM scanner (NT-MDT, Moscow, Russia) [2]. In case of TEM (TECHNAI-20G2, Philips, Holland), a drop of dispersion of IBH-PNPs was placed on a carbon-coated copper grid. The grid subjected to visualization after drying at room temperature, under TEM with an accelerated voltage of 210 kV.

The entrapment efficiency (EE) of prepared nanoparticles was determined by the indirect method. In this method, the nano-formulation (500 μl) was taken and transferred to the upper chamber of nanosep centrifuge tube. The tube was centrifuged at 15,000 rpm for 20 min at -4°C . The supernatant (200 μl) was taken and diluted appropriately. The amount of drug present in the supernatant was determined by UV spectrophotometer at λ_{max} 286 nm [3,4]. The drug loading (DL) was calculated by dividing the amount of total entrapped drug with the total lyophilized nanoparticles weight. The EE & DL calculated by following formulas:

$$\text{Drug EE(\%)} = \frac{\text{Total drug content} - \text{Free drug content}}{\text{Total drug content}} \times 100$$

$$\text{Drug loading(\%)} = \frac{\text{Weight of IBH entrapped within nanoparticles}}{\text{Total weight of prepared nanoparticles}} \times 100$$

2.1.4. In-vitro drug release study

The dialysis membrane technique was employed. The dialysis membrane (Hi-media, molecular weight 12,000–14,000) was soaked overnight in the phosphate buffer solution for its activation. The dialysis tube, filled with 5 mL of re-dispersed IBH-PNPs, was placed in a 150 mL phosphate buffer (pH 7.4) containing beaker and stirred at a constant speed (100 rpm at $37 \pm 0^\circ\text{C}$) using Teflon-coated magnetic bead. The sampling was done at predetermined time intervals up to 72 h from the receptors compartment. Meanwhile, it was replenished with the fresh buffer; maintaining the sink conditions. UV spectrophotometer, at 286 nm, was used to analyze the samples. The experiment was conducted in triplicate; the result was expressed as the average % drug release \pm standard deviation. The order of release and release mechanism, calculated by using the *in-vitro* release data in the following drug releases kinetics: zero order, first order, Higuchi model, and Korsmeyer-Peppas model.

2.1.5. Fourier transforms infrared (FTIR) spectroscopy study

The FTIR study (SHIMADZU 8400, Japan) was carried out for compatibility assessment. In order to understand the interaction, the characteristic bands and peaks of IBH, PLGA, TPGS, Physical mixture, and IBH-PNPs were analyzed. Using a pressed pellet technique, the samples were compressed with potassium bromide (KBr); to form a thin pellet. Then, the pellets were exposed to the IR path length for scanning against the blank KBr background. The scanning range used was from 4000 to 400 cm^{-1} [5].

2.1.6. X-ray diffraction (XRD) study

X-ray diffraction analysis was used to assess the crystallographic structure of IBH inside IBH-PNPs. The XRD fingerprints of IBH, PLGA, physical mixture, and IBH-PNPs were studied; exploiting X-ray diffractometer (Rigaku, Japan) at room temperature. The samples to be analyzed were placed in a rotating sample holder and scanned in a range of 5–60 (2θ) at room temperature [5].

2.1.7. Storage stability

The nanoparticles have a high tendency to agglomerate owing to their large surface area-to-volume ratio, which results in the increase in particle size after long periods of storage. The formulation indicates the instability if there are changes in the following physical appearance: color, odor, taste, and texture. The stability studies of the optimized IBH-PNPs were carried out at room temperature ($25 \pm 2^\circ\text{C}$ and $60 \pm 5\%$ RH) and refrigerated condition ($2 \pm 8^\circ\text{C}$). The critical quality attributes (i.e. particle size, EE, and PDI) were chosen as stability indicating parameters.

2.1.8. Animal study

The Central Animal Ethical Committee of Banaras Hindu University approved the animal study protocols (Approval no-Dean/2018/CAEC/637). The guidelines of CPCSEA (Committee For the Purpose of Control and Supervision of Experiments on Animals), Ministry of Social justice and Empowerment, Government of India, New Delhi, were followed throughout the studies. The male Wistar rats (200–250 g) were placed in the propylene cages, and standard laboratory atmosphere was ensured with a 12 h light/dark cycle. Free access to food and water was ensured for all the animals. The animals were sacrificed by Euthanasia; disposal by incineration.

2.1.8.1. Ex-vivo intestinal permeation study. The non-everted gut sac technique is being used for assessing the intestinal permeation potential of IBH-PNPs across the GIT [5]. The healthy rats were divided into two groups ($n = 3$) and sacrificed by cervical dislocation under ether

anesthesia. The small intestine was isolated by abdominal incision and immediately placed into ice-cold, bubbled (carbogen, 95:5 O_2/CO_2) saline solution. The small intestine, 20–30 cm distal from the pyloric sphincter was then flushed with a physiological saline solution using a blunt end syringe to remove any intestinal content and cut into segments. The IBH solution and IBH-PNPs were filled in the intestinal at 5°C with continuous aeration (carbogen, 95:5 O_2/CO_2) using laboratory aerator. The samples were withdrawn at predetermined time intervals from the receptor compartment (conical flask) and replenished with an equal volume of fresh, pre-warmed buffer solution. The withdrawn samples were sonicated (15 min), filtered through $0.2\mu\text{m}$ membrane filters and suitably diluted in order to analyze the IBH content by spectrophotometer at λ_{max} 286 nm [4,6,7]. The apparent permeability coefficients (P_{app}) for IBH solution and IBH-PNPs were calculated using following formula and expressed in cm^2/s [12].

$$P_{\text{app}} = \frac{\partial Q}{\partial t} \times \frac{1}{AC_0}$$

where, $\partial Q/\partial t$ is the steady-state appearance rate of IBH-PNs/CS in the receiver compartment, A is the exposed intestinal tissue surface area (cm^2) and C_0 is the initial concentration of the IBH in the donor compartment at zero time. The Permeability enhancement ratio for IBH was calculated according to the formula:

2.1.8.2. In-vivo anti-anginal study (single-dose study). Rats were divided in four groups; normal control ($n = 6$), disease control ($n = 6$), test formulation ($n = 6$), marketed formulation ($n = 6$). The test formulation and marketed formulation, equivalent to dose of 1.54 mg/kg, calculated as per dose conversion formula, and administered orally by gavage tube (2 ml) to respective groups 1 h prior to induction of angina.

2.1.8.2.1. Induction of myocardial ischemia. Male wistar rats (200–250g) were anesthetized using isoflurane (inhalation anesthetic) and placed on a heating pad to maintain temperature at 37°C with backs down. The isoflurane (2%) in 100% oxygen at 0.2 L/min was used for maintenance of anesthesia. The lead wires snapped onto the needle electrode ch1 positive, ch2 negative and ground were inserted into left arm, right arm and right leg respectively. After the stabilization of anesthesia, the vasopressin (VP) was injected intravenously at a dosage of 2 IU/kg [28,29]. The ST-wave segment $\geq 1\mu\text{v}$ was considered as an index of myocardial ischemia [29]. The mentioned ischemia induction was used for three consecutive days. After 1 h, the single drug dosing (2 ml IBH-PNPs dispersion or 2 ml dispersed IBH tablet in purified water) was given.

2.1.8.2.2. Measurement of the time to ST-segment depression, duration and severity. The I-Worx Data acquisition and analysis system was used to monitor and assess the electrocardiogram of rats. The vasopressin was injected intravenously and the depression in ST-segment was used as an index of myocardial ischemia recorded by LabScribe software.

2.1.8.2.3. Statistical analysis. All the results were statistically analyzed and expressed as mean \pm standard deviation (SD). The results were compared to control by employing one-way ANOVA, two-way ANOVA, student (unpaired) *t*-test, Tukey test, Bonferonni test using GraphPad Prism Software (version 5.03, GraphPad Software, USA). The level of significance was taken to be $p < 0.01$ and $p < 0.05$.

3. Results and discussion

3.1. Optimization by box-behnkon experimental design (BBD)

A total of 17 experimental runs were obtained through the BBD matrix. The experiments were performed and statistical optimization results were shown in Table 2. The individual as well as interactive effect of independent variables on dependent variables examined as

Table 2
Box-Behnken experimental design matrix.

Run No.	A	B	C	Particle size (nm)	EE%	PDI
1	0	1	1	167.2 ± 10.2	60.0 ± 4.8	0.230 ± 0.036
2	-1	1	0	174.5 ± 2.7	65.7 ± 2.3	0.28 ± 0.027
3	0	0	0	195.2 ± 6.8	72.0 ± 2.7	0.40 ± 0.043
4	-1	-1	0	186.2 ± 3.9	64.0 ± 1.9	0.31 ± 0.029
5	0	0	0	197.9 ± 10.2	64.2 ± 2.2	0.39 ± 0.036
6	0	0	0	199.0 ± 10.8	65.3 ± 3.1	0.41 ± 0.047
7	0	0	0	197.8 ± 9.6	65.0 ± 2.4	0.38 ± 0.029
8	0	-1	0	198.4 ± 7.1	68.0 ± 2.2	0.42 ± 0.072
9	0	1	-1	197.8 ± 4.3	67.3 ± 3.6	0.41 ± 0.048
10	1	1	0	208.1 ± 3.8	72.3 ± 5.3	0.52 ± 0.056
11	1	0	1	203.9 ± 5.3	72.8 ± 3.6	0.46 ± 0.049
12	-1	0	-1	189.1 ± 5.7	66.2 ± 4.1	0.34 ± 0.064
13	-1	0	1	171.6 ± 6.3	55.3 ± 2.8	0.21 ± 0.036
14	0	0	0	197.0 ± 5.7	72.3 ± 4.8	0.38 ± 0.053
15	1	-1	0	226.7 ± 4.8	74.5 ± 2.6	0.55 ± 0.054
16	1	0	-1	238.2 ± 3.6	74.9 ± 2.0	0.53 ± 0.027
17	0	-1	-1	216.6 ± 5.8	71.3 ± 2.1	0.49 ± 0.043

follows:

3.1.1. Influence of independent variables on particle size

The particle size of the prepared IBH-PNPs was obtained in the range of 167.4 ± 10.2 to 238.2 ± 3.6 nm. Based on the lack of fit test, the quadratic model was selected for the statistical analysis. The following polynomial equation can be used to describe the impact of independent variables on particle size:

$$\text{Particle size: } 197.4 + 20.32*A - 10.02*B - 11.66*C + 0.082*A*B - 4.2*A*C - 1.26*B*C + 1.82*A^2 - 2.09*B^2 + 1.53*C^2 \quad (1)$$

The non-significant lack of fit value (0.384; $p > 0.05$), and model F-value 15.41 suggests that the quadratic model is the best fit for describing the significant effect of independent variables on particle size. The R^2 -value (0.954) implies the agreement between predicted and experimental value. Further, the low value of the coefficient of variation (3.06%) indicated a high degree of precision and reliability of the model. The adequate precision is 15.25 while only 4 is desirable. The precision value shows an adequate signal to noise ratio. As per the statistical values obtained, the selected model can be used to navigate the design space.

As per the equation [1], the particle size of IBH-PNPs increases with an increase in polymer amount, owing to its direct influence on the viscosity. When the polymer concentration is increased, the polymer-polymer interactions coupled with the viscosity of dispersed phase which reduces stirring capacity, resulting in poor dispersion and thereby, coarse emulsion forms, that builds larger size polymer particles during diffusion process [8,9]. The monotonous decrease in particle size was observed with an increment in TPGS concentration, which might be due to a reduction in interfacial tension between aqueous and organic phases, resulted in small particles [15]. Additionally, the higher surfactant concentration offers the interfacial stabilization against coalescence to smaller particles [25,26]. Similarly, the organic/aqueous phase ratio is inversely proportional to particle size. By preventing the droplet aggregation as a result of the presence of a large amount of organic solvent, the increase in organic to aqueous phase ratio leads to a decrease in particle. It decreases the polymer concentration as well as viscosity and imparts higher shear stress to break down the emulsion droplets. Except for the polymer amount (because of the direct impact on viscosity), all other variables have a significant negative effect on particle size. There is a little interaction effect between polymer concentration and organic/aqueous ratio (-4.20*A*B).

3.1.2. Influence of independent variables on entrapment efficiency (EE %)

The EE (%) of IBH-PNPs is being achieved in the range of 55.3 ± 2.8 to 74.9 ± 2%. Based on the lack of fit test, the quadratic

model was selected for the statistical analysis of the results. The following polynomial equation could be used to explain the independent variables on EE (%):

$$\text{Entrapment efficiency} = 67 + 6.12*A - 3.37*B - 2.43*C + 0.45*A*B + 2.20*A*C + 0.81*B*C - 1.23*A^2 + 1.17*B^2 - 0.77C^2 \quad (2)$$

The lack of fit value was non-significant (0.6979; $p > 0.05$) with an F-value of 0.39 indicated that the quadratic model is the suitable fit for describing the influence of independent variables on the entrapment efficiency. There is a good correlation between predicted and experimental regression line ($R^2 = 0.82$). Further, the precision and reliability of the model were confirmed by the low value for the coefficient of variation (5.03%) [10]. The adequate precision value is 7.34 (> 4) which indicates there is an adequate signal to noise ratio. Hence, the selected model can be used to navigate the design space.

All other model terms except polymer amount, have a significant negative effect on entrapment efficiency. The highest coefficient value (6.12) of polymer amount suggested that entrapment efficiency would increase with an increase in polymer amount. Whereas the negative values of organic/aqueous phase ratio and TPGS concentration depict that entrapment efficiency would decrease with the increase of these variables.

3.1.3. Influence of independent variables on polydispersity index (PDI)

The IBH-PNPs have shown relatively narrow particle size distribution; indicated by relatively low PDI values. The polydispersity index was obtained in the range of 0.230 ± 0.036 to 0.55 ± 0.056. The low PDI nearer to 0 indicates the relatively homogenous nature of the dispersion of particles. Based on the lack of fit test, the quadratic model was selected for the statistical analysis of the results. The following polynomial was obtained:

$$\text{Polydispersity index} = 0.39 + 0.12*A - 0.041*B - 0.037*C + 0.012*A*B + A*C - 0.014*B*C + 0.012*B^2 \quad (3)$$

The lack of fit value was non-significant (0.1618; $p > 0.05$) for the quadratic model. The higher R^2 value (0.9587) indicated that there is a good correlation between experimental and predicted values. The precision and reliability of the model were established by a low value of the coefficient of variation (7.71%). The adequate precision value is 14.45 (> 4) which indicates there is an adequate signal to noise ratio. Hence, the selected model can be used to navigate the design space.

Except for the polymer amount, other variables i.e. TPGS concentration & organic/aqueous ratio has a significant negative effect on PDI. The increase in PDI value with the increase in polymer amount might be due to the formation of coarse dispersion which forms due to lack of resistive viscous forces, which is supposed to directly affect the emulsification efficiency and produces different sized particles [25,26]. Further, the lack of sufficient TPGS concentration for stabilization of newly formed particles also enhances the particle size distribution. Whereas, an increase in TPGS concentration and organic/aqueous ratio decreases and reducing interfacial tension [2,8].

3.1.4. Optimization of IBH-PNPs using desirability function

It is difficult to optimize a formula taking all the objectives because independent variables might have opposite effects. Therefore, employing the desirability approach, optimization was carried out. All experimental runs were put in Design-Expert®, and the values of the dependent variable predicted employing numerical optimization. The composite desirability of the predicted batch was 0.723 (Table 3). The low bias between predicted results and experimental results, confirmed the suitability of Box-Behnken design [3,13].

3.1.5. Preparation of optimized batches

First, organic phase was prepared by dissolving PLGA (25 mg) and

Table 3

Comparison of experimental and predicted values of optimized IBH-PNPs with its desirability generated by Design Expert®.

Independent Variables		Optimized levels		
Polymer amount (A)		25 mg		
TPGS concentration (B)		0.15%		
Organic phase/aqueous phase ratio (C)		0.66		
Results				
Dependent Variables	Experimental values	Predicted values	Bias	%Error
Particle size (nm)	167.2 ± 10.2	175.08	7.88	4.5%
Entrapment efficiency (%)	60 ± 4.8	66.01	6.01	9.1%
Polydispersity index (PDI)	0.230 ± 0.036	0.28	0.05	17.85
Overall desirability	0.723			
Drug loading (%)	15.92 ± 1.3			
Zeta potential (mv)	-43.73 mv			

Span 80 (0.2 ml) in dichloromethane. Next, the drug solution was obtained by adding IBH (6 mg) in distilled water (0.3 ml). Then, under probe sonication, drug solution was added into the organic phase to obtain primary emulsion (w/o) for 2 min. Next, TPGS was dissolved in water and a solution (0.15%) was obtained. Finally, The primary emulsion (w/o) was dropped into TPGS solution (8 ml) using a syringe under homogenization (12000 RPM) to obtain secondary emulsion (w/o/w). The prepared emulsion (w/o/w) was kept on magnetic stirring overnight for the evaporation of the dichloromethane and then lyophilized.

3.2. Physicochemical characterization of IBH-PNPs

The particle size and polydispersity index was calculated by Photon correlation spectroscopy using Delsa Nano C (Beckman Coulter, USA). The particle size and polydispersity index of optimized batch was found to be 167.26 ± 10.2 nm and 0.230 respectively. The zeta potential of the optimized batch was found to be optimum -43.73 mv. The highly charged nanoparticles are more stable in terms of agglomeration.

The optimized formulation exhibited $60 \pm 4.8\%$ and $15.92 \pm 1.3\%$ entrapment efficiency and drug loading respectively. The surfactant concentration and amount of polymer play an important role in achieving the maximum entrapment. The surface properties of IBH-PNPs were examined by employing transmission electron microscopy and atomic force microscopy. The TEM micrographs of formulation showed spherical shaped, discrete nanosized and uniform size distribution (Fig. 1(A)). The AFM results were analyzed using Nova px control software for roughness (0.333 nm), skewness (0.00815), and

kurtosis (3.19) of nanoparticles. The 2D and 3D images of nanoparticles are shown in Fig. 1 (B). The particles are found to be smooth surface and symmetrical distribution. The obtained results fulfill the ideal properties of nanoparticles [4].

3.3. Fourier transforms infrared (FTIR) spectroscopy study

The FT-IR spectra of the drug revealed characteristic bands at 3414 cm^{-1} (amine), 1209 cm^{-1} (ether), 2833 cm^{-1} (methyl), 1647 cm^{-1} (carbonyl), 1460 cm^{-1} (C=C). The spectra of physical mixture and lyophilized IBH-PNPs revealed bands at 3421 cm^{-1} , 1203 cm^{-1} , 2843 cm^{-1} , 1653 cm^{-1} , and 1456 cm^{-1} . The overlays FTIR spectrum of optimized formulation is shown in Fig. 2(A) suggesting the absence of drug-excipient interaction. The presence of absorption bands of drugs in spectra of formulation confirms that the drug is retained in its original form and there is no chemical interaction.

3.4. X-ray diffraction (XRD) study

The overlays XRD spectra of pure drug (IBH), polymer (PLGA), physical mixture and IBH-PNPs are shown in Fig. 2 (B). The XRD pattern of drug exhibit sharp peaks at angle 8.029, 10.36, 16.106, 17.38, 20.167 26.44 with relative intensity 68.30, 46.03, 49.79, 55.13, 100.00, 43.47 respectively, suggesting the crystalline nature. Further, PLGA (50:50) exhibited characteristic peaks of amorphous nature. The XRD pattern of formulation (IBH-PNPs) resembles the absence of characteristic peaks of crystalline nature, suggesting the amorphous nature of drugs in the system.

3.5. In-vitro drug release study

The retention of drugs within the nanoparticles is critical for sustained drug delivery. Fig. 3 depicts the slow release of IBH from nanoparticles in PBS 7.4 for 72 h. The optimized batch exhibited around $80.02 \pm 2.12\%$ drug released and exhibited burst release (23.82%) in 1hr. The release data was then fitted to various empirical equations to calculate the regression coefficient (R^2) for the kinetic model (8). The highest R^2 value of 0.9210 was observed for the Higuchi model, indicating initial drug concentration in the matrix is much higher than the drug's solubility in the matrix. It might be due to drug entanglement in polymer during the manufacturing process. After an initial burst release, there was a constant slow release of drugs, which attributed to constant drug diffusivity through polymer erosion [21].

3.6. Storage stability study

The changes in the physicochemical properties of the IBH-PNPs during the stability study over 3 months are depicted in Table 4. No significant change was noticed in the physical appearance (*i.e.*, lump

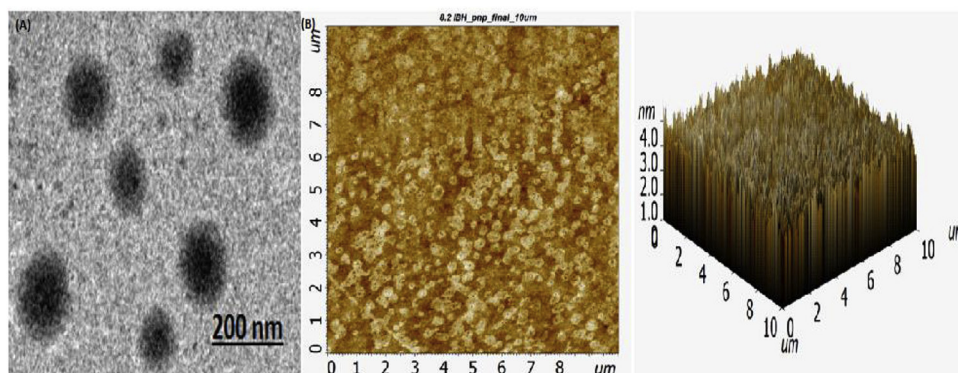


Fig. 1. (A) TEM image of IBH-PNPs (B) 2D and 3D, AFM image of IBH-PNPs.

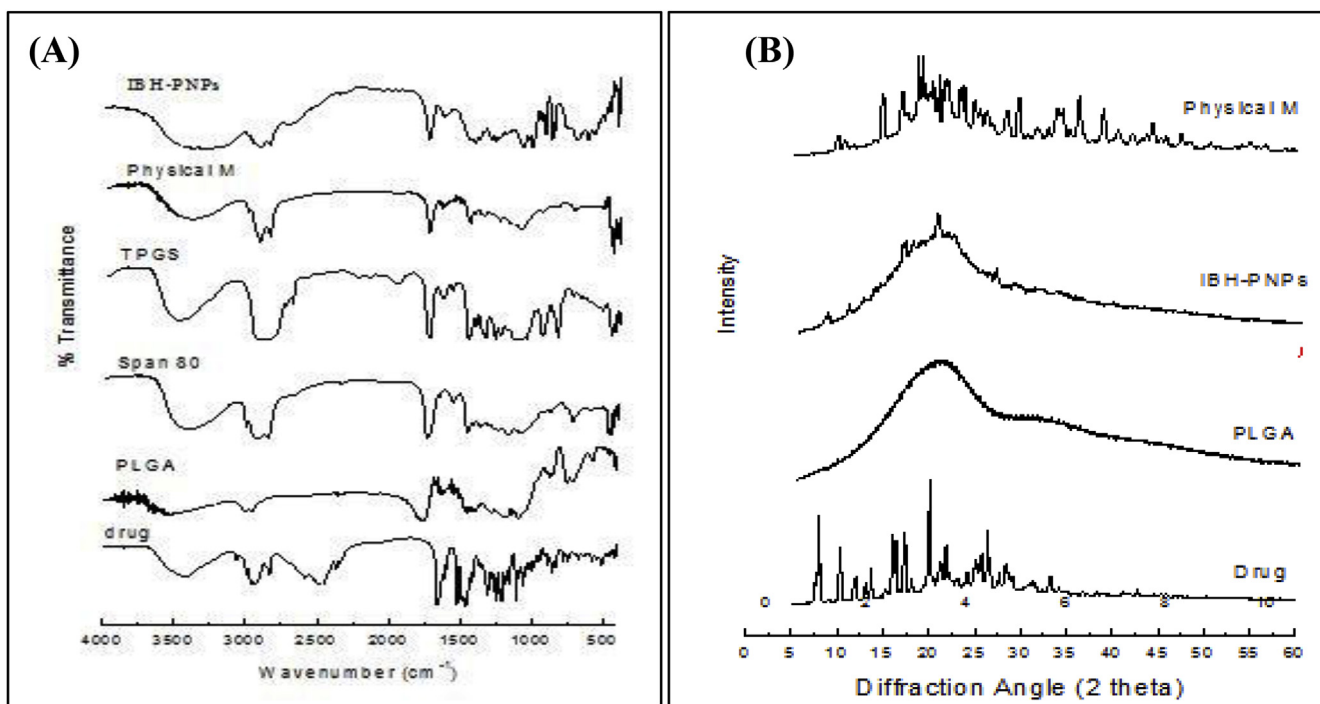


Fig. 2. Overlay graph of (A) FTIR spectra (B) XRD patterns.

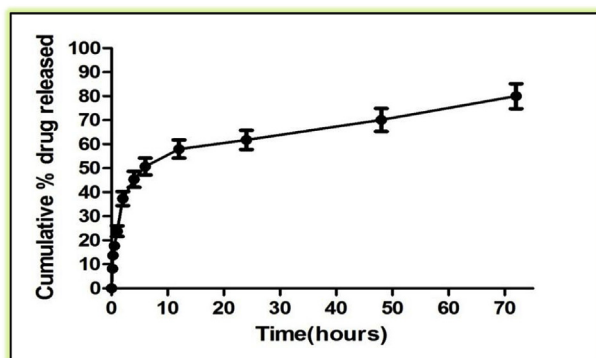


Fig. 3. *In-vitro* drug release profile of IBH-PNPs in phosphate buffer pH 7.4 (vertical bar represent \pm S.D; n = 3).

Table 4
Stability results of IBH-PNPs at room temperature and refrigerated conditions.

IBH-PNPs at room temperature			
Days	Particle Size (nm)	PDI	EE%
0	167.20 \pm 10.2	0.230 \pm 0.036	60.53 \pm 4.8
30	172.32 \pm 6.3	0.235 \pm 0.015	56.25 \pm 2.2
60	178.02 \pm 5.2	0.239 \pm 0.018	53.13 \pm 2.01
90	182.32 \pm 4.9	0.244 \pm 0.013	51.23 \pm 3.4
IBH-PNPs at refrigerated conditions			
0	167.20 \pm 10.2	0.230 \pm 0.036	60.53 \pm 4.8
30	169.02 \pm 4.21	0.232 \pm 0.014	57.78 \pm 3.4
60	172.54 \pm 4.36	0.237 \pm 0.017	56.56 \pm 4.5
90	176.32 \pm 3.3	0.238 \pm 0.019	54.02 \pm 4.1

formation and discoloration) at mentioned environmental conditions during the study. The depositions appeared on the base of the container were easily re-dispersible on mere shaking. The insignificant change ($p > 0.05$) in particle size, entrapment efficiency and PDI of IBH-PNPs was noticed [8, 9].

3.7. Animal studies

3.7.1. *Ex-vivo* intestinal permeation study

The *ex-vivo* intestinal permeation of IBH-PNPs and pure IBH solution along with their apparent permeability coefficient (Papp) at pH 7.4 is depicted in Fig. 4. The permeation of IBH-PNPs was significantly higher ($p < 0.05$) at each time point; approximately 1.859 fold across the rat intestinal tissue compared to pure IBH solution (Fig. 4 (A) and B). The intestinal permeability coefficients for IBH solution and IBH-PNPs were found to be $0.2826 (\pm 0.023) \times 10^{-5}$ and $0.5253 (0.036) \times 10^{-5}$ cm/s, respectively. The higher permeation of IBH-PNPs can be justified by the large surface area furnished by their nano-sized structure which might have facilitated more absorption [10]. The particles of size range (< 500 nm) are absorbed by intestinal enterocytes through endocytosis and TPGS presence on the surface help in crossing the cellular barrier [27]. Additionally, the surfactant used in formulation of IBH-PNPs (*i.e.*, TPGS) improves mucoadhesion which might have helped in increasing the intestinal permeability [10].

3.7.2. *In-vivo* anti-anginal activity

3.7.2.1. Effect of Ivabradine Hydrochloride on ST-Segment depression time, duration and onset. The IBH-PNPs in dose of (1.54 mg/kg) produced significant increase ($p < 0.05$) in the onset of ST-segment depression and significantly decreases ($p < 0.05$) its duration compared to disease control group (Fig. 5). The marketed IBH tablet (1.54 mg/kg) also produced significant effect in the increase in onset and decrease in duration of ST-segment depression but for first day only, after that its effect was statistically non-significant ($p > 0.05$) in disease control group.

3.7.2.2. Effect of Ivabradine Hydrochloride on severity of ST-segment depression induced by vasopressin. The IBH-PNPs (1.54 mg/kg) produced a significant decrease ($p < 0.05$) in the ST-segment height at time of 0.5, 1, 3, and 6 min, respectively after vasopressin injection (Fig. 6). The marketed IBH tablet also produced a significant decrease in ST-segment height but for one day only, after that it produced a non-significant ($p > 0.05$) decrease compared to disease control group. The three days significant action of IBH-PNPs owing to its sustained release

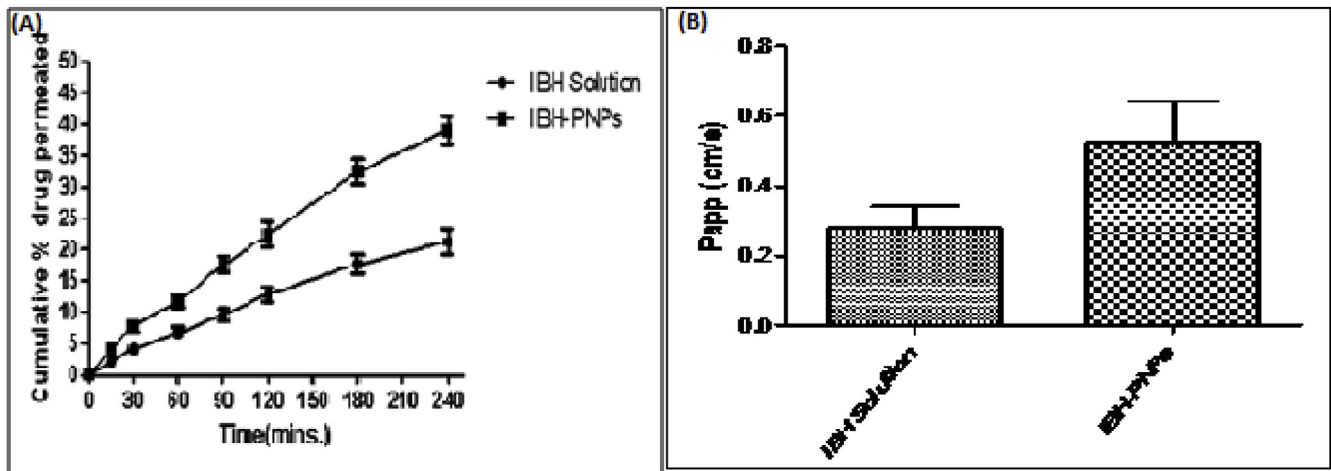


Fig. 4. (A) *Ex-vivo* permeation study of IBH-PNPs and IBH solution across rat intestinal membrane. (B) Apparent permeability coefficients (Papp) for IBH from IBH-PNPs and IBH solution. Error bars represent mean \pm SD; n = 3, the results were found to be significant (p < 0.05), Unpaired student t-test used for comparison.

property discussed in *in-vitro* section.

4. Discussion

The nanotechnology has been utilized to overcome the problem of marketed formulation. The nanotechnology based polymeric

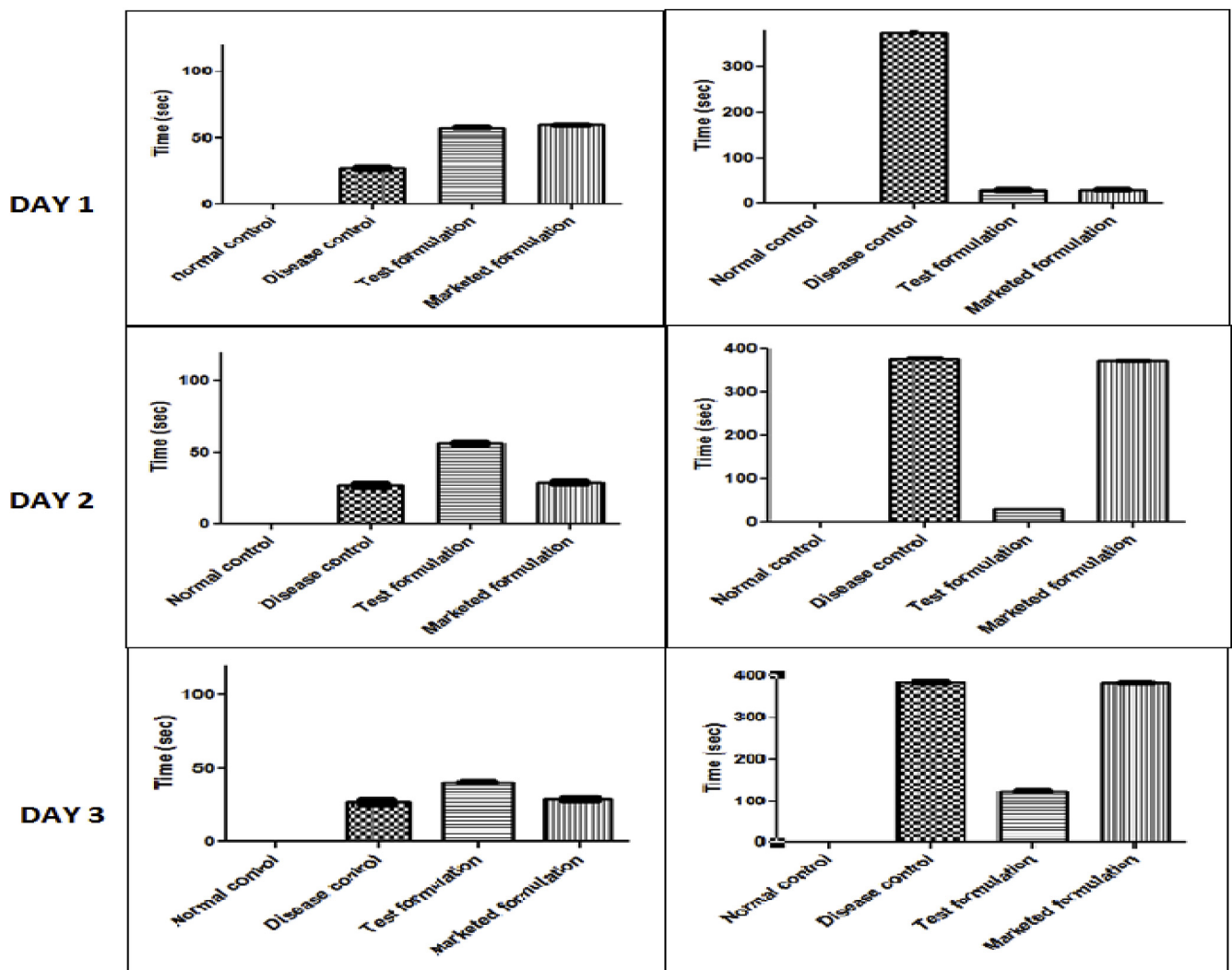


Fig. 5. Day wise effect of IBH-PNPs and IBH tablet (Marketed formulation) in terms of onset of ST-segment depression (A,C,E) and duration of ST-segment depression (B,D,F) in rats; one-way ANOVA followed by Tukey's test, error bars represent \pm SEM; n = 6. (*p < 0.05).

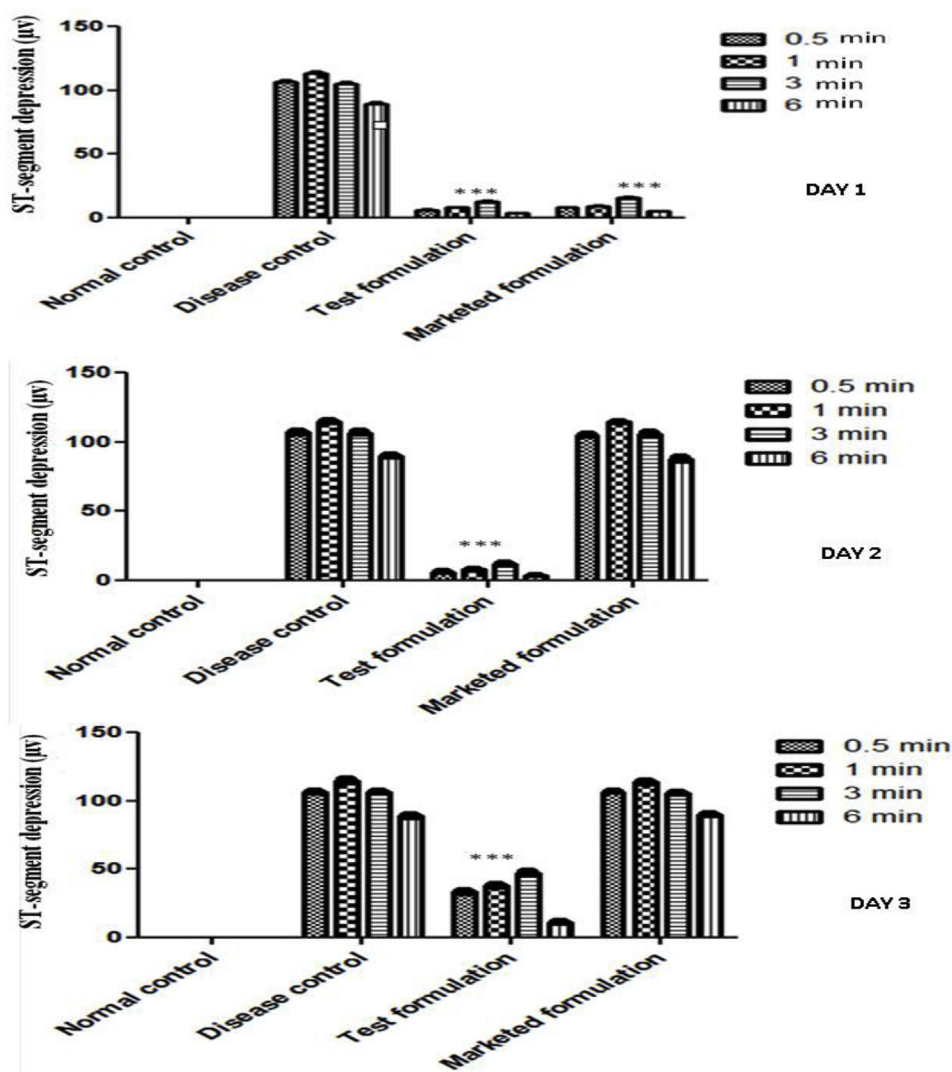


Fig. 6. Comparison of effects produced by IBH-PNPs (formulation) and IBH Tablet (marketed formulation) for three consecutive days. Values are expressed as mean \pm SEM; $n = 6$ rats; *** $P < 0.05$, comparing to disease control group: by two-way ANOVA and Bonferroni post hoc test.

nanoparticles have been prepared by double emulsion method using PLGA (50:50) as polymer and TPGS as surfactant, and applying Box-Behnken experimental design for the optimization of independent formulation variables. The effects of independent variables on dependent variables (*i.e.* particle size, entrapment efficiency, and PDI) have been explained by mathematical polynomial equation. The quadratic model was found to be significant for the analysis of impact on all the dependent variables. As per the data generated by model, the particle size of IBH-PNPs increases with the increase in polymer amount which could be attributed to increase in the viscosity of the dispersed phase, which reduces the stirring rate and applied shear required to form a small globule size emulsion. As a result, coarse emulsion forms that result in larger size particles [2,25]. Additionally, A density difference might have been created between two phases at higher polymer concentration which retards the faster diffusion of the solvent (DCM) into the external aqueous phase, and increases the collisions between the particles due to enhanced contact that leads to bigger coacervates [2,14]. The polymer amount has a positive effect (entrapment increases with increase in polymer amount) on entrapment efficiency due to its direct effect on viscosity. The higher polymer amount offers viscous diffusional barrier which curtails the drug diffusion into the external aqueous phase and thereby, provides higher entrapment. Inversely, higher TPGS concentration lowers the EE by decreasing the interfacial

tension that promotes the partition and hence increases the solubility of the drug into the aqueous phase during preparation [17,24]. Similarly, the reduction in EE with an increase in organic/organic phase ratio was seen due to a substantial reduction in the viscous diffusional barrier [18]. Except for polymer concentration (positive effect) other variables exhibit negative effect (*i.e.* PDI decrease with the increase of polymer amount) on PDI. The increase in PDI with increase of polymer concentration can be justified by same mechanism as in case of particle size *i.e.* coarse emulsion formation due to increase in viscosity which reduces the stirring rate and leads to the particles of different sizes. The decrease in PDI with the increase of TPGS may be attributed to the reduction of the interfacial tension within the system which makes the system homogeneous and PDI goes down [18].

The extended-release behavior of IBH from IBH-PNPs can be correlated with homogeneous encapsulation within the nanoparticles, which hinders the faster mobilization from the polymeric matrix and controls the release [16,20]. The high zeta potential value makes the IBH-PNPs more stable due to the columbic repulsion forces arising from their surface charge [2]. These forces help in overcoming the van der Waals attractive forces and prevent aggregation. The narrow PDI can be well correlated with the kurtosis and skewness values obtained from the AFM study which shows the uniform particles size distribution in the system. The particle size obtained from dynamic light scattering is

correlated well with the particle size exhibited by morphology study (i.e. TEM and AFM). The *in-vitro* release study showed the initial burst release which might be due to the drug present on the surface of the nanoparticles. The Higuchi model justifies the release behavior of IBH-PNPs i.e. the initial burst release followed by sustained behavior. The prepared IBH-PNPs are highly permeable through intestinal tissue which can be attributed to the large surface area furnished by their nano-sized structure, which might have facilitated more absorption due to muco-adhesive property of TPGS [3]. The reduction in dose of IBH was also noticed in IBH-PNPs which may be due to reduction in hepatic first pass metabolism as IBH-PNPs would preferably be absorbed by the lymphatic system before reaching the systemic circulation. Additionally, due to presence of TPGS coating the permeability of IBH-PNPs must have been higher than marketed tablet [3,10,11]. IBH-PNPs release the drug by erosion and diffusion in a sustained manner which gave three days of action. Throughout three days, prepared IBH-PNPs produced a significant effect by increasing the onset, decreasing duration and severity of vasopressin induced ST-segment depression in wistar rats.

5. Conclusions

Ivabradine Hydrochloride loaded polymeric nanoparticles were prepared and evaluated by various techniques. Prepared nanoparticles were found to be more permeable via intestine compared to marketed formulation. The anti-anginal study of nanoparticles showed significant effects for three consecutive days. The dose (1.54 mg/kg) of IBH given in form of IBH-PNPs found to be equivalent to 3 days dose of IBH tablet. Hence, prepared IBH-PNPs were found to have sustained release profile for longer period of time, reducing the dosing frequency and enhanced the permeability.

Declaration of competing interest

The authors have no conflict of interest.

Acknowledgment

Authors are thankful to institute for providing the necessary facilities. I would like thank to Central instrument facility, Indian Institute of Technology (BHU) for characterization of synthesized compounds.

Abbreviations

BBD	Box banker design
CHD	Coronary heart disease
DL	Drug loading
EE	Entrapment efficiency
FTIR	Fourier transforms infrared
IBH	Ivabradine Hydrochloride
IBH-PNPs	Ivabradine Hydrochloride polymeric nanoparticles
NPs	Nanoparticles
PBS	Phosphate buffer saline
PDI	Polydispersity index
PLGA	Poly lactic-co-glycolic acid
RSM	Response surface methodology
TPGS	D- α -tocopherol polyethylene glycol
XRD	X-ray diffraction

Appendix A. Supplementary data

Supplementary data to this article can be found online at <https://doi.org/10.1016/j.jddst.2019.101337>.

Funding

The formulation development and characterization studies were supported by a research grant from the Department of Pharmaceutical Engineering and Technology, Indian Institute of Technology (Banarasi Hindu University), Varanasi- 221005, India.

References

- [1] B. Gajra, P.R. Patel, C. Dalwadi, Formulation, optimization and characterization of cationic polymeric nanoparticles of mast cell stabilizing agent using the Box–Behnken experimental design, *Drug Dev. Ind. Pharm.* 42 (2016) 747–757.
- [2] P. Chaubey, R.R. Patel, B. Mishra, Development and optimization of curcumin-loaded mannosylated chitosan nanoparticles using response surface methodology in the treatment of visceral leishmaniasis, *Expert Opin. Drug Deliv.* 11 (2014) 1163–1181.
- [3] H.K. Dewangan, T. Pandey, L. Maurya, S. Singh, Rational design and evaluation of HBsAg polymeric nanoparticles as antigen delivery Carriers, *Int. J. Biol. Macromol.* 111 (2018) 804–812.
- [4] R.R. Patel, G. Khan, S. Chaurasia, N. Kumar, B. Mishra, Rationally developed core–shell polymeric-lipid hybrid nanoparticles as a delivery vehicle for cromolyn sodium: implications of lipid envelop on *in vitro* and *in vivo* behaviour of nanoparticles upon oral administration, *RSC Adv.* 5 (2015) 76491–76506.
- [5] S. Singh, A.K. Dobhal, A. Jain, J.K. Pandit, S. Chakraborty, Formulation and evaluation of solid lipid nanoparticles of a water soluble drug: zidovudine, *Chem. Pharmaceutical bulletin* 58 (2010) 650–655.
- [6] A.W. Alani, J.R. Robinson, Mechanistic understanding of oral drug absorption enhancement of cromolyn sodium by an amino acid derivative, *Pharm. Res. (N. Y.)* 25 (2008) 48–54.
- [7] A. Gandhi, S. Jana, K.K. Sen, *In-vitro* release of acyclovir loaded Eudragit RLPO® nanoparticles for sustained drug delivery, *Int. J. Biol. Macromol.* 67 (2014) 478–482.
- [8] S. Chaurasia, N. Kumar, R.R. Patel, B. Mishra, Optimization of parameters for the fabrication of curcumin loaded polymeric nanoparticles using taguchi robust design, *Adv. Sci. Lett.* 20 (2014) 1028–1038.
- [9] S. Chaurasia, P. Chaubey, R.R. Patel, N. Kumar, B. Mishra, Curcumin-polymeric nanoparticles against colon-26 tumor-bearing mice: cytotoxicity, pharmacokinetic and anticancer efficacy studies, *Drug Dev. Ind. Pharm.* 42 (2016) 694–700.
- [10] M. Tariq, M.A. Alam, A.T. Singh, Z. Iqbal, A.K. Panda, S. Talegaonkar, Biodegradable polymeric nanoparticles for oral delivery of epirubicin: *in vitro*, *ex vivo*, and *in vivo* investigations, *Colloids Surf., B* 128 (2015) 448–456.
- [11] L. Barthe, J. Woodley, S. Kenworthy, G. Houin, An improved everted gut sac as a simple and accurate technique to measure paracellular transport across the small intestine, *Eur. J. Drug Metab. Pharmacokinet.* 23 (1998) 313–323.
- [12] M.S. Freag, Y.S. Elnaggar, O.Y. Abdallah, Development of novel polymer-stabilized diosmin nanosuspensions: *in vitro* appraisal and *ex vivo* permeation, *Int. J. Pharmaceutics.* 454 (2013) 462–471.
- [13] R.R. Patel, N. Kumar, G. Khan, S. Chaurasia, B. Mishra, Investigation of critical variables of core–shell polymer lipid hybrid nanoparticles by using plackett–Burman screening design, *Adv. Sci. Lett.* 20 (2014) 923–932.
- [14] A.F. Ribeiro, R.L. de Oliveira Rezende, L.M. Cabral, V.P. de Sousa, Poly ϵ -caprolactone nanoparticles loaded with *Uncaria tomentosa* extract: preparation, characterization, and optimization using the Box–Behnken design, *Int. J. Nanomed.* 8 (2013) 431–439.
- [15] D. Sharma, D. Maheshwari, G. Philip, R. Rana, S. Bhatia, M. Singh, R. Gabrani, S.K. Sharma, J. Ali, R.K. Sharma, S. Dang, Formulation and optimization of polymeric nanoparticles for intranasal delivery of lorazepam using Box–Behnken design: *in vitro* and *in vivo* evaluation, *BioMed Res. Int.* (2014) 1–14.
- [16] A. Budhian, S.J. Siegel, K.I. Winey, Haloperidol-loaded PLGA nanoparticles: systematic study of particle size and drug content, *Int. J. Pharmaceutics.* 336 (2007) 367–375.
- [17] Z. Rahman, A.S. Zidan, M.J. Habib, M.A. Khan, Understanding the quality of protein loaded PLGA nanoparticles variability by Plackett–Burman design, *Int. J. Pharmaceutics.* 389 (2010) 186–194.
- [18] S.A. Guhagarkar, V.C. Malshe, P.V. Devarajan, Nanoparticles of polyethylene sebacate: a new biodegradable polymer, *AAPS PharmSciTech* 10 (2009) 935–944.
- [19] A.B. Solanki, J.R. Parikh, R.H. Parikh, Formulation and optimization of piroxicam proniosomes by 3-factor, 3-level Box–Behnken design, *AAPS PharmSciTech* 8 (2007) 43–55.
- [20] R.R. Patel, S. Chaurasia, G. Khan, P. Chaubey, N. Kumar, B. Mishra, Highly water-soluble mast cell stabiliser-encapsulated solid lipid nanoparticles with enhanced oral bioavailability, *J. Microencapsul.* 33 (2016) 209–220.
- [21] B. Wilson, M.K. Samanta, K. Santhi, K.S. Kumar, M. Ramasamy, B. Suresh, Chitosan nanoparticles as a new delivery system for the anti-Alzheimer drug tacrine, *Nanomedicine: NBM (NMR Biomed.)* 6 (2010) 144–152.
- [22] K.Y. Win, S.S. Feng, Effects of particle size and surface coating on cellular uptake of polymeric nanoparticles for oral delivery of anticancer drugs, *Biomaterials* 26 (2005) 2713–2722.
- [23] A. des Rieux, V. Fievez, M. Garinot, Y.J. Schneider, V. Pr eat, Nanoparticles as potential oral delivery systems of proteins and vaccines: a mechanistic approach, *J. Control. Release* 116 (2006) 1–27.
- [24] H.K. Dewangan, L. Maurya, A. Srivastava, S. Singh, Hepatitis B antigen loaded biodegradable polymeric nanoparticles: formulation optimization and *in-vivo*

- immunization in BALB/c mice, *Curr. Drug Deliv.* 15 (8) (2018) 1204–1205.
- [25] A.F. Ribeiro, R.L. de Oliveira Rezende, L.M. Cabral, V.P. de Sousa, Poly ϵ -caprolactone nanoparticles loaded with *Uncaria tomentosa* extract: preparation, characterization, and optimization using the Box–Behnken design, *Int. J. Nanomed.* 8 (2013) 431–441.
- [26] D. Sharma, D. Maheshwari, G. Philip, R. Rana, S. Bhatia, M. Singh, R. Gabrani, S.K. Sharma, J. Ali, R.K. Sharma, S. Dang, Formulation and optimization of polymeric nanoparticles for intranasal delivery of lorazepam using Box–Behnken design: in vitro and in vivo evaluation, *BioMed Res. Int.* (2014) 1–14.
- [27] K.Y. Win, S.S. Feng, Effects of particle size and surface coating on cellular uptake of polymeric nanoparticles for oral delivery of anticancer drugs, *Biomaterials* 26 (2005) 2713–2722.
- [28] Y. Hirata, H.M. Mabuchi, T. Sasaki, H. Maruyama, Y. Kase, S. Takeda, M. Aburada, Antianginal effects of lercanidipine or methacholine on the vasopressin induced angina model in rats, *Biol. Pharm. Bull.* 28 (2005) 811–816.
- [29] J. Ikeda, M. Matsubara, K. Yao, Effects of benidipine in a rat model for experimental angina, *Yakugaku Zasshi* 126 (2) (2006) 1377–1381.
- [30] M.F. Zambaux, F. Bonneaux, R. Gref, P. Maincent, E. Dellacherie, M.J. Alonso, P. Labrude, C. Vigneron, Influence of experimental parameters on the characteristics of poly(lactic acid) nanoparticles prepared by a double emulsion method, *J. Control. Release* 50 (1–3) (1998) 31–40.